RSC Advances

ROYAL SOCIETY OF CHEMISTRY

www.rsc.org/advances

RSC Advance

ARTICLE

Quick synthesis of zeoliticimidazolate framework microflowers with enhanced surpercapacitor and electrocatalytic performances

Received 00th January 20xx,

Accepted 00th January 20xx

DOI: 10.1039/x0xx00000x

www.rsc.org/

Daojun Zhang [a], Huaizhong Shi [a], Renchun Zhang [a], Zirui Zhang [a], Nan Wang [a], Junwei Li [a], Baiqing Yuan*[a], HelongBai[b], Jingchao Zhang*[a]

Novel zeolitic imidazolate framework-67 (ZIF-67) microflowers were synthesized by a quick and simple method without using any template or surfactant. Enhanced specific capacitance (188.7 F g^{-1} at 1A g^{-1}) and good cycle stability (remaining 105% after 3000 cycles) of ZIF-67 microflowers are observed in aqueous KOH electrolytes, which could be ascribed to the high chemical and thermal stabilities,large BET surface area,and small ion-transport (OH^-) resistance of the hierarchical microflowers structure. In addition, the as-prepared ZIF-67 microflowers exhibited good electrocatalytic activity toward the reduction of H_2O_2. The obtained sensor also presented good reproducibility, high stability and wide linear range. This work suggests that ZIF materials would offer a promising candidate for the potential applications in surpercapacitor and electroanalysis.

1.Introduction

Metal–organic frameworks (MOFs) represent a new class of tunable materials that have shown great potential applications in heterogeneous catalysis, gas storage, nonlinear optics, nanomedicine, and energy storage [1–11]. Investigations into the use of MOFs as supercapacitors electrode materials have expanded in recent years, the MOFs themselves have unique structures incorporating pseudo-capacitive redox centers that can be directly used as a new type of electrode materials[5]. However, studies into the direct use of MOFs as supercapacitor electrodes are rather rare and more challenging due to the weak stability and poor electrical conductivity of most MOFs. Very recently, Yaghi*et al.* reported a series of graphene-doped MOFs nanocrystals fabricated a symmetric supercapacitor, and it was found that the Zr-MOF exhibited a high capacitance of 726 F g^{-1} at a current density of 0.88 mA cm^{-3} (6.95 mA g^{-1})[12]. Wang *et al.* demonstrated a strategy to design andfabricate a flexible MOF-based supercapacitor (PANI-ZIF-67-CC)[13].The results showed that the PANI-ZIF-67-CC delivers anextraordinary areal capacitance of 2146 mF cm^{-2} at 10 mVs^{-1}.Wei *et al.* reported a Ni-based and a Zn-doped Ni-based MOFs with high capacitances[14, 15].However, it is unclear why specifically 6 M KOH electrolyte was used, and the long-term stability of the Ni-MOF structure is uncertain. MOFs including Co-, Co-Zn-, Zn-, In-, Ni-, and Cd-based materials have also been investigated [16–22], however, most reports showed low capacitances.

The most important is that to increase the stability of MOFs in water and alkaline solution. To overcome the disadvantages, recently, a large number of MOFs with chemical and thermal stabilities, such as ZIF-8, ZIF-67 and MIL-101[23–37], have been reported. The redox behavior of metal Co(II) ions inside the ZIF-67 could provide a transport pathway for electrons, we think ZIF-67 is a suitable electrode material for surpercapacitor and electrocatalyst. It is well accepted that pseudocapacitors store charge in the first few nanometres from the surface, so the hierarchical flower-like would increase redox metal centers, and thereby would increase the pseudocapacitance. Thus, it is quite necessary to synthesize MOF material with a unique hierarchical flower-like structure, which can provide more active sites and short diffusion paths for charge carriers, which may endow the materials with enhanced electrochemical properties.

Herein, we synthesized ZIF-67 with hierarchical flower-like structure, the constructed amperometric sensor from the combination of ZIF-67 with traditional electrode showed a linear range for the detection of H_2O_2 from 2.5 μM to 1.08 mM with a correlation coefficient of 0.9926. Moreover, ZIF-67 may be a relatively good candidate of electrochemical capacitors with a specific capacitance up to 188.7 F g^{-1} at a current density of 1 A g^{-1} and a long cycle life which can maintain 105% of initial specific capacitance after 3000 cycles at a current density of 2 A g^{-1}. These results strongly show that the as-made ZIF-67 hierarchical flower-like structure display excellent electrochemical properties for supercapacitor and electrochemistry sensor.

[a]*College of Chemistry and Chemical Engineering, Anyang Normal University, Anyang 455002, China. Tel: +86 03722900040, E-mail:baiqingyuan1981@126.com (B. Yuan), zjc19830618@126.com (J. Zhang)*
[b]*College ofChemistry, Jilin University, Changchun 130012, China.*
†Electronic Supplementary Information (ESI) available: [details of any supplementary information available should be included here]. See DOI: 10.1039/x0xx00000x

2. Experimental section

2.1 Materials synthesis

2-methylimidazole was purchased from Aldrich and used without further purification. Deionized water was used throughout all the experiments. In a typical synthesis, 174.6mg $Co(NO_3)_2 \cdot 6H_2O$ (0.6mmol) and 738.9 mg 2-methylimidazole (9.0 mmol) were dissolved in 9 mL of deionized water, the mixed solution was stirred for 5 h at room temperature, then the resulting purple precipitates were collected by centrifuging, washed several times with distilled water and absolute methanol, and finally vacuum-dried at 60 °C for 12 h.

2.2 Materials characterization

The resultant phase of the microflower ZIF-67particles was determined by X-ray diffraction by X-ray diffraction (XRD) on a Philips X'pert Pro X-ray diffractometer with Cu Ka radiation and operated at 40 kV and 40 mA. The surface morphology was measurements by field-emission scanning electron microscopy (FESEM) on a Hitachi SU8010 instrument.

2.3 Electrochemical sensor electrode preparation and measurement

The electrochemical measurements were examined on an electrochemical workstation (CHI 760D, Chenhua, Shanghai, China) using a carbon paste electrode (CPE) as working electrode, a platinum coil as counter electrode, and a Ag/AgCl electrode as reference electrode, respectively. To prepare the ZIF-67 modified electrode, 2.0 mg of the as-prepared material was dispersed in 1.0 mL water to give suspension by ultrasonicating. A 5.0 µL of the suspension was dip-coated onto CPE and the electrode was then dried in the atmosphere.

2.4 Electrochemical supercapacitor electrode preparation and measurement

All the electrochemical experiments were carried out in a standard three-electrode system at room temperature. A saturated calomel electrode (SCE) and a platinum foil were used as the reference and counter electrodes, respectively. The working electrodes were typically fabricated by mixing 80% of active material, 10% of acetylene black, and 10% of polyvinylidene fluoride (PVDF), using N-methyl-2-pyrrolidone (Aldrich) as solution to yield a slurry. Then the slurry was pressed on the nickel foam current collector (1 cm×1 cm) and dried in vacuum at 100 °C for 10 h. The electrochemical measurements were carried out by an electrochemical analyzer system, CHI 760D (Chenhua, Shanghai, China). The electrochemical performance of the electrode was analyzed using cyclic voltammetry (CV) and galvanostatic charge-discharge measurements in 1 M KOH aqueous solution in the potential window from 0 to 0.46 V.

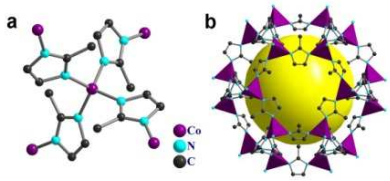

Fig. 1 (a)The coordination environment and (b) SOD-type structure of ZIF-67.

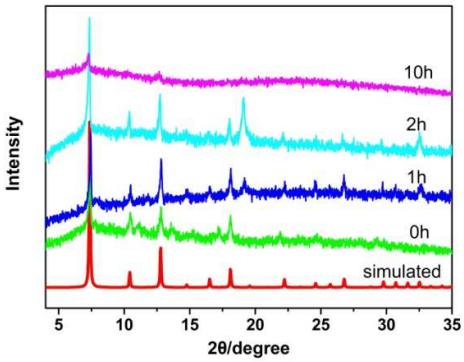

Fig. **2** PXRD patterns of the as-synthesized ZIF-67 as well as samples treated with 1M KOH aqueous solutions at different time at room temperature.

3. Results and discussion

In this MOF, each cobalt ion is coordinated with four nitrogen atoms from four different 2-methylimidazolate ligands and every ligand bridge two Co centers and further assembles into a sodalite (SOD) topology framework (Fig.1). ZIF-67 exhibits large surface area and high stability in water [33].The identity and purity of the samplesare confirmed by similarities between the experimental X-ray powder diffraction (PXRD) spectra, furthermore, our experiment shows ZIF-67 has good corrosion resistance of KOH aqueous solutions (Fig.2), all these merits are important applied for the electrode material of supercapacitors. Fig. 3a and b show the FESEM images of ZIF-67 at different magnifications, revealing that the as-synthesized ZIF-67 product is entirely composed of microspheres with a diameter of 1–2 µm (Fig. 3a). Further observation suggests that the individual microflower is actually 3D flowerlike hierarchical assemblies of interconnected nanoparticles about tens of nanometers in length (Fig. 3b).

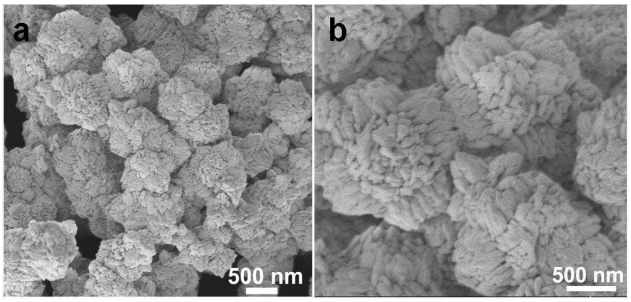

Fig. **3** The FESEM images of ZIF-67 at low (a) and high (b) magnifications.

The CV experiments within a 0~0.55 V range at a scan rate from 5 to 50 mV s^{-1} for ZIF-67 was presented in Fig. 4. As shown in Fig. 4a, obviously, a pair of strong redox peaks is in each voltammogram suggesting that the capacity of ZIF-67 are mainly based on Faradaic redox reactions. At a low scan rate of 5 mV s^{-1}, the anodic peak at 0.37 V is due to the oxidation process, and the cathodic peak at about 0.27 V is related to its

reverse process. The electrochemical capacitance of ZIF-67 originates from the Faradic redox reaction of Co(II) ions (Co^{2+}/Co^{3+} redox couple) in the framework, and probably mediated by the OH^- ions in the alkaline electrolyte. The positive sweeps of the CV curves of ZIF-67 are not symmetrical with thecorresponding negative sweeps, which might be caused by polarization and ohmic resistance during the Faradaic process.

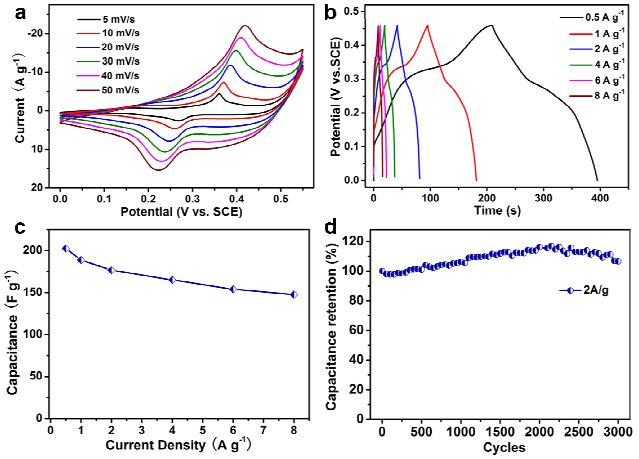

Fig. **4** Electrochemical performance characterization of ZIF-67 hierarchical flower-like structure: (a) CV curves of ZIF-67 modified electrode at various sweeping rates ranging from 5 to 50 mV s^{-1}. (b) Galvanostatic charge-discharge curves of ZIF-67 at different current densities. (c) The specific capacitances at different current densities from 0.5 to 8A g^{-1}. (d)Cycling performance of ZIF-67 hierarchical flower-like structure at a constant current density of 2 A g^{-1}.

The current-density dependence of specific capacitance is calculated from above discharge curves and plotted in Fig.4b. Apparently, the ZIF-67 hierarchical structure active electrode delivers specific capacitance of 202.6, 188.7, 176.6, 165.0, 153.9 and 147.6 F g^{-1} at current densities of 0.5, 1, 2, 4, 6, and 8 A g^{-1}, respectively. In addition, the hierarchical flower-like structure sample stillretains the highest capacitance of ~72.9 % after the current densities increasing from 0.5 to 8 A g^{-1} (Fig.4c). The results in this work are higher than that previously reported mesoporous 437-MOF (81 F g^{-1} at 1 A g^{-1}) [18]. Furthermore, the values are comparable to the typical cobalt oxide supercapacitor, such as $CoMoO_4$nanorods (62.8 F g^{-1} at 1 A g^{-1}), $MnMoO_4$nanorods (9.7 F g^{-1} at 1 A g^{-1}) and hierarchical $MnMoO_4/CoMoO_4$ nanowires (187.1 F g^{-1} at 1 A g^{-1}) [38] and is even higher than nanocomposite, such as $CoMoO_4$/MWCNTs (170 F g^{-1} at 2 A g^{-1}) [39], but less than that of the supercapacitor based on NiO@$CoMoO_4$nanocomposite[40] and $CoMoO_4$-3D graphene hybrid (NSCGH)[41]electrodes. The long-term cycle ability is also key factor in practical applications of supercapacitors. The cycling performance test indicates that the capacitance of this device slightly increases with the number of charge–discharge cycles. The increasing capacitance with the cyclic charge–discharge process might be due to activation of the ZIF-67 porous structure with time. This makes the porous structure of ZIF-67 in full contact with the electrolyte. The final specific capacitance of theZIF-67 hierarchical flower-like structure is 105% of its initial value after 3000 cycles (Fig. 4d). These results suggest that ZIF-67 hierarchical flower-like nanostructure may be a promising candidate for high-performance supercapacitors.

To evaluate the specific surface area and the porosity of the hierarchical flower-like structure, the N_2 sorption property was studied and shown in Fig.S1, it reveals a typical type IV adsorption isotherm with a H3-type hysteresis loop at a relative pressure of 0.5–1.0, indicating the presence of the mesoporous structure. The pore size distribution exhibits a relatively wide peak centered at 14.5 nm, and the BET specific surface area is 412.87m^2/g. The specific surface area of hierarchical flower-like structure is higher than the previously reported ZIF-67 nanoparticles witha BET of 316 m^2/g[30]. In order to comparethe electrochemical performanceof ZIF-67with different morphologies, the normal ZIF-67 nanocrystal was synthesized according to a previous reported [30], the SEM image is shown in Fig.S2, and electrochemical performance characterization for surpercapacitor was also studied (Fig. S3). At the same condition, the ZIF-67 nanocrystals active electrode delivers specific capacitance of 155.57, 149.77, 141.99, 132.38, 127.20 and 121.10 g^{-1} at the discharge current densities of 0.5, 1, 2, 4, 6, and 8 A g^{-1}, respectively. Remarkably, the electrochemical properties of our obtained ZIF-67 hierarchical flower-like structure are better than that of ZIF-67 nanocrystals with regular structure. The enhancement in electrochemical capacitance of the as-obtained ZIF-67 hierarchical flower-like structure should be ascribed to the unique hierarchical structure and large BET surface area, which endows massive electroactive sites for electrochemical reactions and more efficient penetration of electrolyte ions (OH^-) into the electroactive electrode materials.

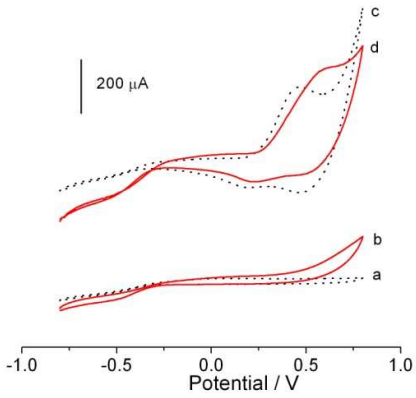

Fig. **5** CVs of bare CPE (a, b) and ZIF-67-CPE (c, d) in the absence (a, c) and presence (b, d) of 10 mM H_2O_2 in 0.1 M NaOH.

Fig.5 shows the CVs of bare CPE (a, b) and ZIF-67-CPE (c, d) in the absence (a, c) and presence (b, d) of 10 mM H_2O_2 in 0.1 M NaOH. For bare CPE, only a small reduction peak with the

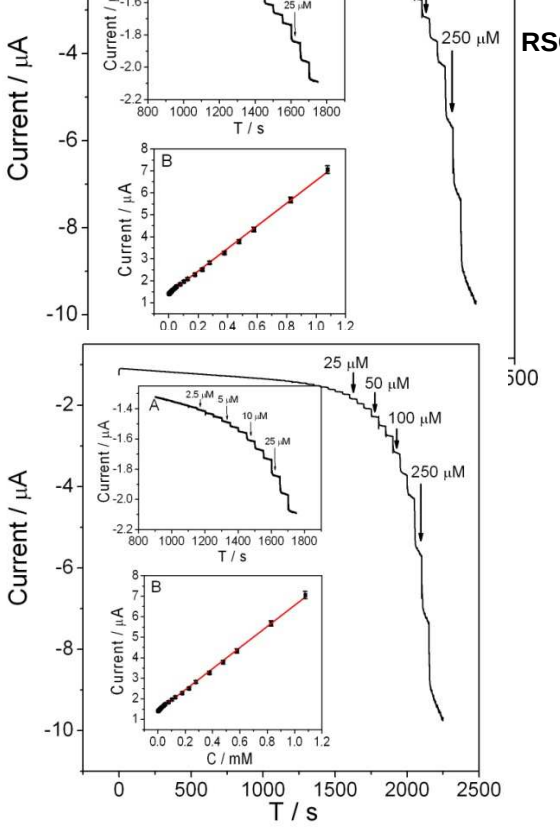

Fig. **6**Amperometric sensing of H_2O_2 by successive addition of H_2O_2 for ZIF-67-CPE at -0.3 V in 0.1 M NaOH. Inset: (A), amperometric response at low concentration of H_2O_2; (B), plot of amperometric response versus the concentration of H_2O_2 from 2.5 μM to 1.08 mM.

Based on the ZIF-67, nonenzymatic H_2O_2 sensor was developed, and the sensing property was evaluated by amperometric i–t curve. Fig.6 depicts the typical amperometric response of ZIF-67-CPE electrode upon successive additions of H_2O_2 into a continuously stirring 0.1 M NaOH solution at a potential fixed at -0.3 V (optimal signal-noise ratio). As shown in Fig.6, upon addition of H_2O_2, a rapid increase in the reduction current was observed, indicating a fast response attributed to the excellent electrocatalytic activity of ZIF-67-CPE. The sensor presented a wide linear range from 2.5 μM to 1.08 mM (R^2=0.999) with a detection limit of 2.5 μM (S/N=3) which is lower than Si/GO sensor (2.6 μM) [42], polynucleotide-templated silver nanoclusters/graphene sensor (3 μM) [43], silver-nanoparticle-decorated graphene sensor (5 μM) [44].

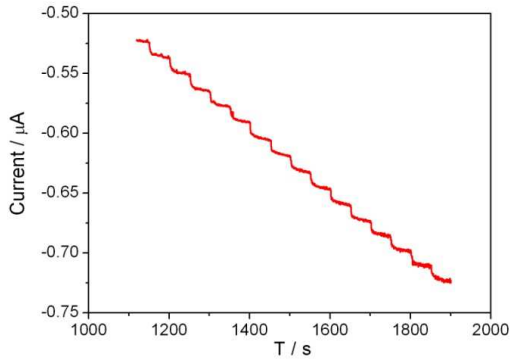

Fig. **7** Repeatable test of ZIF-67-CPE by successive addition of 3 μM H_2O_2.

graphene/Nafion/Azure I/Au nanoparticles sensor (10 μM) [45], and graphene wrapped Cu_2O nanocubes sensor (20.8 μM) [46].

The reproducibility and stability of the sensor were performed by measuring the amperometric response to H_2O_2. The average relative standard deviation (RSD) was not more than 3.9% for fifteen successive determinations using the same sensor, and 4.7% for six different sensors which were fabricated independently by the same procedure described in Experimental, indicating the good reproducibility of the method (Fig.7). The long-term stability of the sensor was examined by a continuous and successive operation. The amperometric response retained about 98% of its initial value to H_2O_2 after continuous running for 1600 s (Fig.8). The as-prepared sensor was stored in air, and the amperometric response was recorded every twelve hours. It was found that the current response is approximately 96% of the originally measured value after two weeks. The good operation performances of the presented sensors could be attributed to the high stability of the ZIF-67 in alkaline solution. The selectivity of the sensor was also examined by CVs. The results indicated that the common interfering substances including AA, UA, glucose, and ethanol did not interfere with the determination of H_2O_2.

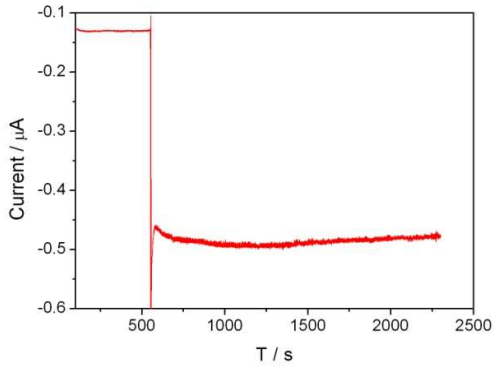

Fig. **8** Long-term amperometric test of ZIF-67-CPE with 80 μM H_2O_2.

4. Conclusions

Herein, we demonstrated ZIF-67hierarchical flower-like structure can be synthesized by a simple method without using any template or surfactant. Enhanced specific capacitance and good cycle stability are observed in aqueous KOH electrolyte for ZIF-67hierarchical structure. In addition, the as-prepared ZIF-67 hierarchical structure exhibited good electrocatalytic activity toward the oxidation of H_2O_2. The sensors presented good reproducibility, excellent electrocatalytic activities, high stability and wide linear range. These impressive results presented here show great potential in designing a new type of MOF structure in the future for promising applications in the high performance energy storage systems and electrocatalyst.

Acknowledgments

Financial supports from the National Science Foundation of China (Nos. 21405005, U1404208, 21301009), the Project Sponsored by the Scientific Research Foundation for the Returned Overseas Chinese Scholars, State Education Ministry, the Project of Science and Technology Department of Henan Province (Nos. 122102310521, 122102210460, 142102210586) and Foundation of Henan Educational Committee (No.15A150031, 15A150002, 13B150893) are gratefully acknowledged. We gratefully acknowledge Prof. Qisheng Huo and A.P. Yong Fan for their helpful discussion.

References

1R. J. Kuppler, D. J. Timmons, Q. R. Fang, J. R. Li, T. A. Makal, M. D. Young, D. Q. Yuan, D. Zhao,W. J. Zhuang and H. C. Zhou, *Coord. Chem. Rev.*, 2009, **253**, 3042.
2P. Ramaswamy, N. E. Wong and G. K. H. Shimizu,*Chem. Soc. Rev.*, 2014, **43**, 5913.
3S. L. Li and Q. Xu, *Energy Environ. Sci.*, 2013, **6**, 1656.
4A. Morozanand F. Jaouen, *Energy Environ. Sci.*, 2012, **5**, 9269.
5F. S. Ke, Y. S. Wu and H. X. Deng, *J. Solid State Chem.*, 2015, **223**,109.
6D. F. Wu, Z. Y. Guo, X. B. Yin, Q. Q. Pang, B. B. Tu , L. J. Zhang,Y. G. Wang and Q. W. Li, *Adv. Mater.*, 2014,**26**, 3258.
7J. M. Zheng,J. Tian,D. X. Wu,M. Gu, W. Xu,C. M. Wang, F. Gao,M. H. Engelhard, J. G. Zhang,J. Liu and J. Xiao, *Nano Lett.*, 2014, **14**, 2345.
8Y. Gong,H. F. Shi,P. G. Jiang,W. Hua and J. H. Lin, *Cryst. Growth Des.*, 2014, **14**, 649.
9J. W. Zhang,H. T. Zhang,Z. Y. Du,X. Q. Wang,S. H. Yu and H. L. Jiang, *Chem. Commun.*,2014, **50**, 1092.
10S. B. Wang, Y. D. Hou, S. Lin and X. C. Wang, *Nanoscale*, 2014, **6**, 9930.
11M. Jahan, Q. L. Bao and K. P. Loh, *J. Am. Chem. Soc.*, 2012, **134**, 6707.
12K. M. Choi, H. M. Jeong, J. H. Park, Y. B. Zhang, J. K. Kang and O. M. Yaghi,*Acs Nano*, 2014, **8**,7451.
13L.Wang, X. Feng, L.T. Ren, Q. H. Piao, J. Q. Zhong, Y. B. Wang, H.W. Li, Y. F. Chen, B. Wang, *J. Am. Chem. Soc.* 2015, 1**37**, 4920.
14J. Yang, P. X. Xiong, C. Zheng, H. Y. Qiu and M. D. Wei, *J. Mater. Chem. A*, 2014, **2**, 16640.
15J. Yang, C. Zheng, P. X. Xiong, Y. F. Li and M. D. Wei, *J. Mater. Chem. A*, 2014, **2**,19005.
16N. Campagnol, R. Romero-Vara, W. Deleu, L. Stappers, K. Binnemans, D. E. De Vos, and J. Fransaer, *ChemElectroChem*, 2014, **1**,1182.
17Y. Gong, J. Li, P. G. Jiang, Q. F. Li and J. H. Lin, *Dalton Trans.*, 2013,**42**, 1603.
18M. Du, M. Chen, X. G. Yang, J. Wen, X. Wang, S. M. Fang and C. S. Liu, *J. Mater. Chem. A*, 2014, **2**, 9828.
19A. Borenstein, O. Fleker, S. Luski, L. Benisvy and D. Aurbach,*J. Mater. Chem. A*, 2014, **2**, 18132.
20R. Díaz, M. G. Orcajo, J. A. Botas, G. Calleja and J. Palma,*Mater. Lett.*, 2012, **68**,126.
21D. Y. Lee, S. J. Yoon, N. K. Shrestha, S. H. Lee, H. Ahn and S. H. Han,*Micropor. Mesopor. Mater.*, 2012, **153**,163.
22D. Y. Lee, D. V. Shinde, E. K. Kim, W. Lee, I.-W. Oh, N. K. Shrestha, J. K. Lee and S. H. Han,*Micropor. Mesopor. Mater.*, 2013, **171**, 53.
23A. Phan, C. J. Doonan, F. J. Uribe-Romo, C. B. Knobler,M. O'Keeffe and O. M.Yaghi, Acc. Chem. Res., 2010, **43**, 58.
24B. Wang, A. P. Côté, H. Furukawa, M. O'Keeffe and O. M. Yaghi, *Nature*, 2008, **453**, 207.
25K. S. Park, Z. Ni, A. P. Côté, J. Y. Choi, R. D. Huang, F. J. Uribe-Romo, H. K. Chae, M. O'Keeffe and O. M. Yaghi, *PANS*, 2006, **103**, 10186.
26R. Banerjee, A. Phan, B. Wang, C. Knobler, H. Furukawa, M.O'Keeffe and O. M. Yaghi, *Science*, 2008, **319**, 940.
27B. L. Chen, Z. X. Yang, Y. Q. Zhu and Y. D. Xia, *J. Mater. Chem. A*, 2014, **2**,16811.
28Y. C. Pan, Y. Y. Liu, G. F. Zeng, L. Zhao and Z. P. Lai,*Chem.Commun.*, 2011, **47**, 2071.
29M. Tu, C. Wiktor, C. Rösler and R. A. Fischer, *Chem.Commun.*, 2014,**50**, 13258.
30J. F. Qian, F. Sun and L. Z. Qin, *Mater. Lett.*, 2012, **82**, 220.
31N. L. Torad, R. R. Salunkhe,Y. Q. Li, H. Hamoudi, M. Imura, Y. Sakka, C. C. Hu and Y. Yamauchi,*Chem. Eur. J.*, 2014, **20**,7895.
32Y. C. Pan, D. Heryadi, F. Zhou, L. Zhao, G. Lestari, H. B. Su and Z. P. Lai, *CrystEngComm*, 2011, **13**, 6937.
33T. T. Xing, Y. B. Lou, Q. L. Bao and J. X. Chen, *CrystEngComm*, 2014, **16**, 8994.
34W. Xia, J. H. Zhu, W. H. Guo, L. An, D. G. Xia and R. Q. Zou, *J. Mater. Chem. A*, 2014, **2**,11606.
35J. Shao, Z. M. Wan, H. M. Liu, H. Y. Zheng, T. Gao, M. Shen, Q. T. Qu and H. H. Zheng, *J. Mater. Chem. A*, 2014, **2**, 12194.
36N. L. Torad, M. Hu, S. Ishihara, H. Sukegawa, A. A. Belik, M. Imura, K. Ariga, Y. Sakka and Y. Yamauchi,*Small*, 2014, **10**, 2096.
37R. B. Wu, X. K. Qian, X. H. Rui, H. Liu, B. L. Yadian, K. Zhou, J. Wei, Q. Y. Yan, X. Q. Feng, Y. Long, L. Y. Wang and Y. Z. Huang,*Small*, 2014, **10**, 1932.
38L. Q. Mai, F. Yang, Y. L. Zhao, X. Xu, L. Xu and Y. Z. Luo,*Nature Commun.*, 2011, **2**, 381.
39Z. Xu, Z. Li, X. Tan, C. M. B. Holt, L. Zhang, B. S. Amirkhiz and D. Mitlin, *RSC Adv.*, 2012,**2**, 2753.
40X. J. Ma, L. B. Kong, W. B. Zhang, M. C. Liu, Y. C. Luo and L. Kang,*RSC Adv.*, 2014, **4**, 17884.
41X. Z. Yu, B. G. Lu and Z. Xu, *Adv. Mater.*, 2014, **26**, 1044.
42Y. Huang and S. F. Y. Li, *J. Electroanal. Chem.*, 2013, **690**, 8.
43Y. L. Xia, W. H. Li, M. Wang, Z. Nie, C. Y. Deng and S. Z. Yao, *Talanta*, 2013, **107**, 55.
44A. M. Golsheikh, N. M. Huang, H. N. Lim, R. Zakaria and C. Y. Yin, *Carbon*, 2013, **62**, 405.
45Y. L. Zhang, Y. P. Liu, J. M. He, P. F. Pang, Y. T. Gao and Q.F. Hu, *Electrochim. Acta*, 2013, **90**, 550.
46M. M. Liu, R. Liu and W. Chen,*Biosens. Bioelectron.*, 2013, **45**, 206.

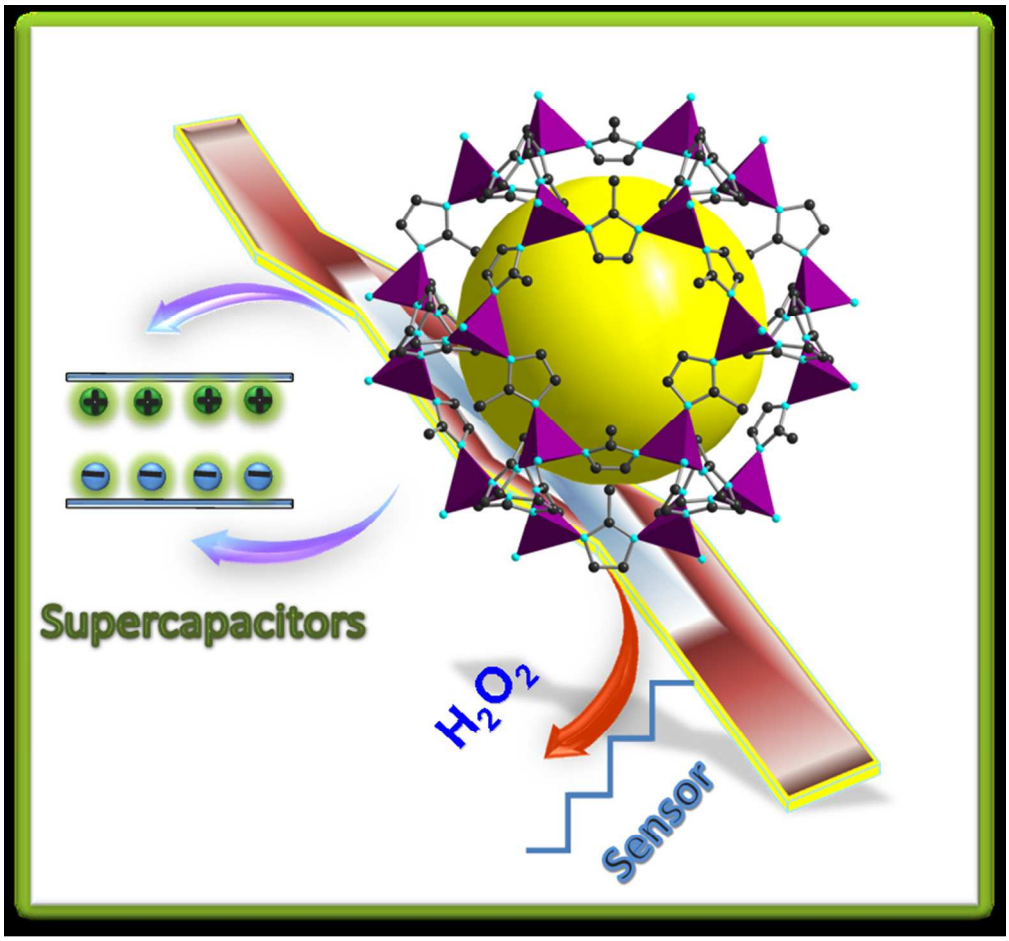

142x132mm (150 x 150 DPI)